# Quantification of measurement uncertainty in the sequential determination of Pb-210 and Po-210 by liquid scintillation counting and alpha-particle spectrometry

**3 AUTHORS**, INCLUDING:

GENERAL PAPER

# Quantification of measurement uncertainty in the sequential determination of $^{210}$Pb and $^{210}$Po by liquid scintillation counting and alpha-particle spectrometry

**Chang-Kyu Kim · Paul Martin · Aleš Fajgelj**

**Abstract** Methodologies for the quantification of measurement uncertainties associated with the determination of $^{210}$Pb- and $^{210}$Po-specific activities by liquid scintillation counting (LSC) and alpha-particle spectrometry are presented, and are demonstrated using the soil reference material IAEA-326. Major contributors to the combined uncertainty associated with the measurement result of $^{210}$Pb were the uncertainties of net count rates in the $^{210}$Pb energy region of the sample spectrum and in the $^{210}$Bi energy region of the blank spectrum. The predominant sources of uncertainty in the measurement of $^{210}$Po were the uncertainties of net count rates in the regions of interest of $^{209}$Po and $^{210}$Po. The relative standard uncertainty of $^{210}$Po exponentially increases with the time interval between the sampling date and the separation date of Po, and this effect is strongly dependent on the $^{210}$Po/$^{210}$Pb activity ratio. When the specific activity of $^{210}$Pb is much higher than that of $^{210}$Po in the sample, the relative standard uncertainty of the $^{210}$Po determination increases significantly within a short time interval between the sampling date (or reference date) and the separation date of Po in samples.

**Keywords** $^{210}$Pb · $^{210}$Po · Measurement uncertainty · Liquid scintillation counting · Alpha-particle spectrometry

## Introduction

Polonium-210 and $^{210}$Pb are naturally occurring radionuclides with half-lives of 138.38 days and 22.3 years,

respectively. Both radionuclides are ubiquitously distributed in the rocks and soils of the earth's crust, and in the atmosphere and natural waters as a result of the decay of $^{222}$Rn. Technologically enhanced sources of $^{210}$Po and $^{210}$Pb include effluents and tailings from the mining industry, particularly in uraniferous areas, the disposal of radium-rich products such as phosphogypsum, and dust from blast furnaces. Because of this widespread distribution, both radionuclides also enter food chains through direct uptake, ingestion, or inhalation. $^{210}$Pb and $^{210}$Po have often been determined in a wide variety of samples in order to study environmental processes [1, 2] and their impact on human health through radiation exposure [3].

The results of several recent proficiency tests organized by the International Atomic Energy Agency (IAEA) have demonstrated that a number of laboratories are still experiencing difficulty in obtaining reliable results for $^{210}$Pb and/or $^{210}$Po determination in environmental matrices [4, 5]. This is, in part, due to the limited number of methods available for their determination (the most commonly used being gamma-ray spectrometry or beta counting for $^{210}$Pb and alpha-particle spectrometry for $^{210}$Po [6]), and technical difficulties with some of these methods (for example, the low energy of the $^{210}$Pb peak in the gamma-ray spectrum). In addition, there is a general lack of suitable, recently characterized reference materials for use in quality control.

To assure the comparability and usefulness of measurement data, the determination results of $^{210}$Pb- and $^{210}$Po-specific activity are normally corrected for ingrowth and decay to the sampling date (or reference date), particularly in cases where the time interval between the sampling and measurement dates is long [7]. In performing the decay correction of the data, changes in measurement uncertainty associated with the corrections should also be

C.-K. Kim (✉) · P. Martin · A. Fajgelj
International Atomic Energy Agency,
Agency's Laboratories, Seibersdorf and Headquarters,
Wagramer Strasse 5, 1400 Vienna, Austria
e-mail: c.k.kim@iaea.org

taken into account. Before some international guides on uncertainty evaluation were published [8–10], the uncertainty in radioactivity measurement was often expressed by the standard deviation of repeated measurements or was given by the square root of the number of counts, which, however, reflects only the counting statistics. Recently, García-Orellana and García-León [11] reported that the relative uncertainty of $^{210}$Pb exponentially increased with the time interval between $^{210}$Po measurements when the activity of $^{210}$Pb was determined by measuring the ingrowth of $^{210}$Po from $^{210}$Pb after radiochemical separation. However, a combined uncertainty evaluation considering all possible sources of uncertainty was not discussed.

Vreček et al. [12] described in detail the evaluation of the measurement uncertainty in the determination of $^{210}$Pb and $^{210}$Po using a gas proportional counter and alpha-particle spectrometry. However, the authors did not elaborate on uncertainty sources that may eventually appear in decay correction to the sampling date, in spite of the fact that the uncertainty of $^{210}$Po could increase with the time interval between the measurement date and the sampling date due to its relatively short half-life (138.38 days).

When carrying out determinations of $^{210}$Pb and $^{210}$Po, the analyst also needs to consider the possible effects of disequilibrium in the sample. As the decay chain from $^{226}$Ra to $^{210}$Po involves several elements, it is quite common for different sample types to exhibit differences of orders of magnitude in their degrees of disequilibrium. For example, rainwater samples commonly have $^{210}$Po/$^{210}$Pb activity ratios of approximately 0.1 [1, 13], while animal tissue samples may have ratios of 10 or even larger [14, 15]. This can affect considerably the allowable delay period between sampling and analysis, and the effect on the uncertainty of the ingrowth and decay corrections.

The purpose of this work was to identify and quantify all uncertainty sources which can appear in the measurement of $^{210}$Pb and $^{210}$Po by liquid scintillation counting (LSC) and alpha-particle spectrometry, including correction to the sampling date. In this paper, it is also presented how the combined uncertainty in the calculation of $^{210}$Po activity on the sampling date depends on the ratio of $^{210}$Po/$^{210}$Pb-specific activities on the sampling date (or the reference date in the particular case of the analysis of a reference material).

## Materials and methods

### Description of the method

Often, low levels of $^{210}$Pb are determined from the measurement of $^{210}$Po using alpha-particle spectrometry after

the ingrowth of $^{210}$Po in a $^{210}$Pb fraction obtained by radiochemical separation [6]. This method is very sensitive. However, it requires a delay period for ingrowth of $^{210}$Po from $^{210}$Pb. Alternatively, $^{210}$Pb can be determined by counting $^{210}$Bi using LSC or a gas proportional counter after the formation of secular equilibrium between $^{210}$Pb and $^{210}$Bi [16]. However, this method also needs at least 20 days to allow the $^{210}$Pb and $^{210}$Bi to reach equilibrium.

In the method described here, $^{210}$Pb is directly measured by LSC without waiting for $^{210}$Pb to reach equilibrium with $^{210}$Bi, saving analysis time. Polonium-210 is measured by alpha spectrometry. It is expected that this method can be used for the rapid measurement of $^{210}$Pb and $^{210}$Po in environmental samples.

### Calibration procedure for the determination of $^{210}$Pb using LSC

#### Preparation of calibration sources

As shown in Fig. 1, a known activity of $^{210}$Pb standard solution (NIST, SRM4337, USA), which is in secular equilibrium with the progeny $^{210}$Bi and $^{210}$Po, and the mass of stable Pb carrier (30 mg) were taken in 10 mL of 2 mol L$^{-1}$ HCl solution and then loaded onto a Sr-resin column (3 g of Sr-resin, 100–150 μm, inner ∅: 10 mm, Eichrom, Tec.). The column was washed with 80 mL of 2 mol L$^{-1}$ HCl and the washing solution was combined with the effluent to obtain a pure $^{210}$Bi fraction (Fig. 1①). The column was rinsed with 20 mL of 2 mol L$^{-1}$ HCl. This last portion of 20 mL 2 mol L$^{-1}$ HCl was discarded to avoid overlapping between the $^{210}$Bi and $^{210}$Po portions (Fig. 1②), and the column was washed with 25 mL of 6 mol L$^{-1}$ HNO$_3$ (Fig. 1③). The polonium was eluted with 60 mL of 6 mol L$^{-1}$ HNO$_3$ (Fig. 1④). The lead was eluted with 60 mL of 6 mol L$^{-1}$ HCl (Fig. 1⑤). The Bi, Po, and Pb fractions (Fig. 1①, ④, ⑤) were, respectively, evaporated to dryness. Each portion of $^{210}$Bi and $^{210}$Po was dissolved in 1 mL of 6 mol L$^{-1}$ HNO$_3$, and then, respectively, transferred into 20 mL polyethylene vials coated with PTFE and mixed with 14 mL of Insta-Gel Plus liquid scintillation cocktail (PerkinElmer, USA). The Pb fraction was evaporated three times with 2 mL of 65% HNO$_3$. The residue was dissolved in 20 mL of 1 mol L$^{-1}$ HNO$_3$. After adding 0.4 g of oxalic acid while warming, the pH of solution was adjusted to 3–5 with NH$_4$OH to form a Pb-oxalate precipitation. The precipitate was filtered on a pre-weighed filter paper (∅ 24 mm), washed three times with 1 mL water and 2 mL of ethanol, and then dried in an oven at 40–50°C. After cooling, the precipitate was weighed to determine the chemical recovery of lead. The
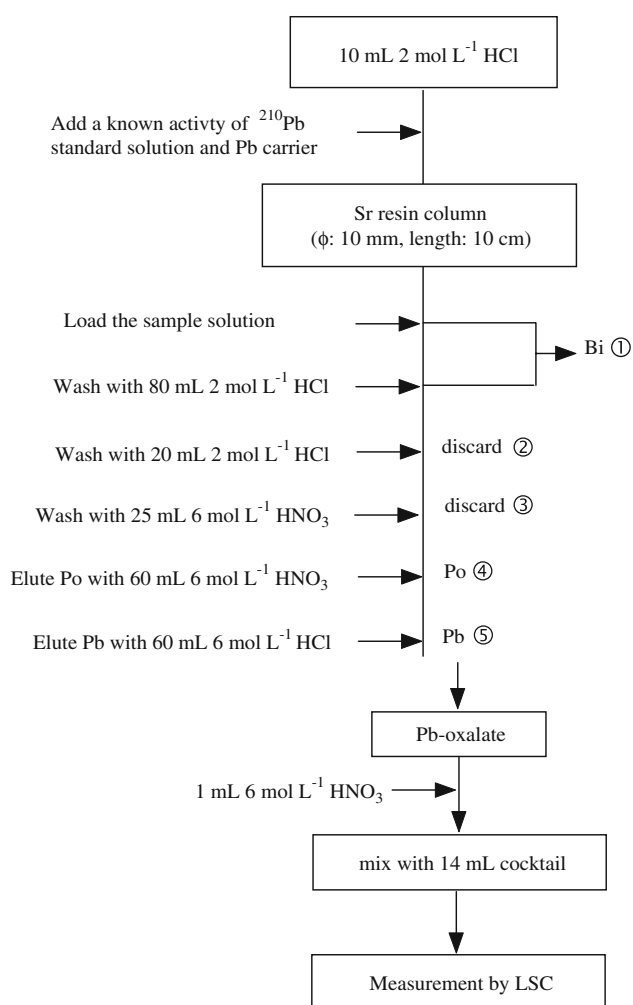
**Fig. 1** Schematic diagram for the sequential separation of $^{210}$Bi, $^{210}$Po, and $^{210}$Pb for the preparation of calibration sources: ① Bi fraction, ② and ③ washing step, ④ Po fraction and ⑤ Pb fraction

lead oxalate precipitate was quantitatively transferred into a liquid scintillation vial together with the filter, and 1 mL of 6 mol L$^{-1}$ HNO$_3$ was added into the vial to dissolve the precipitate. The solution was then mixed with 14 mL of Insta-Gel Plus liquid scintillation cocktail (PerkinElmer, USA). The three vials (for $^{210}$Pb, $^{210}$Bi, and $^{210}$Po) were counted using LSC (Quantulus 1220, PerkinElmer) to set up windows for $^{210}$Pb and $^{210}$Bi, until the counting statistic uncertainty was less than 1%.

*Setting windows for $^{210}$Pb and $^{210}$Bi*

The specific activity of $^{210}$Pb was determined by LSC with the double energetic window method [17]. This method permits the direct determination of $^{210}$Pb without waiting for the ingrowth of $^{210}$Po from $^{210}$Pb.

As shown in Fig. 2a, the lower limit for the $^{210}$Pb energy region (window A) was set at channel 115 to avoid the counts caused by chemiluminescence in the cocktail, while the upper limit was set at channel 320, where the $^{210}$Pb peak ends. The lower limit for the $^{210}$Bi energy region (window B) was set at channel 320, and the upper limit was set at channel 410 to avoid interference from the $^{210}$Po peak.

*Separation of $^{210}$Po and $^{210}$Pb from soil IAEA-326 using Sr-resin*
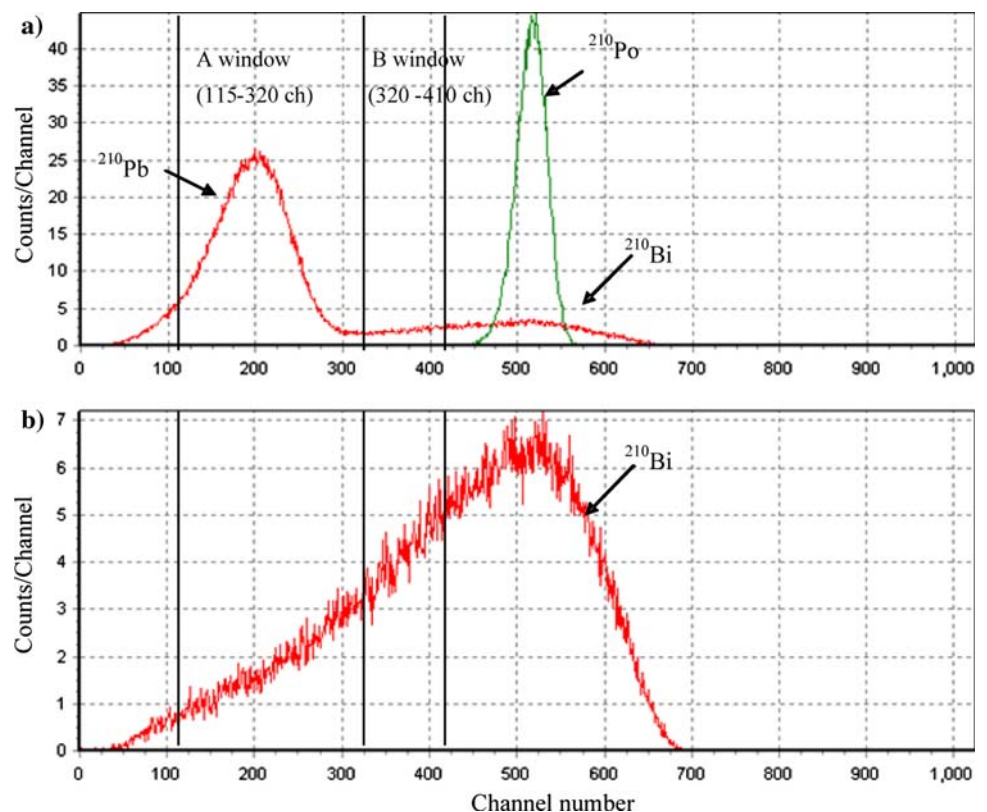
A test portion of 1.0 g (as dry weight) of soil reference material IAEA-326 was weighed into the PTFE vessel of a microwave oven. After adding Pb carrier (30 mg) and $^{209}$Po tracer, 3 mL of 65% HNO$_3$ and 2 mL of 40% HF were added to the sample. The test portion was digested at 150°C for 15 min and then at 190°C for 25 min in a microwave oven (MLS-Ethos Plus, MLS GmbH, Germany), taking into consideration the volatility of polonium. The test solution was then transferred to plastic centrifuge tubes and centrifuged for 10 min. The supernatants were transferred to PTFE beakers. The residues were transferred back into the microwave containers with 3 mL of 65% HNO$_3$, and 2 mL of 40% HF was added. The residue was digested in a microwave oven using the same program as mentioned above. The test solutions were combined with the supernatants and 0.1 g H$_3$BO$_3$ was added and then evaporated with three portions of 5 mL of 65% HNO$_3$ to remove the HF. The residue was dissolved in 30 mL of 2 mol L$^{-1}$ HCl and then loaded onto a Sr-resin column (3 g of Sr-resin (100–150 μm), inner ⌀: 10 mm), which was preconditioned in advance with 100 mL of 2 mol L$^{-1}$ HCl. The columns were rinsed with 100 mL of 2 mol L$^{-1}$ HCl and 25 mL of 6 mol L$^{-1}$ HNO$_3$ to remove interfering elements. Polonium was eluted with 60 mL of 6 mol L$^{-1}$ HNO$_3$ and then lead was eluted with 60 mL of 6 mol L$^{-1}$ HCl [17]. Polonium fractions were carefully evaporated to dryness. The residues were taken up with 10 mL of 0.5 mol L$^{-1}$ HCl and the pH of the solution was adjusted to 2 using 6 mol L$^{-1}$ NaOH. Polonium was auto-deposited onto a silver disc at 90°C for 90 min with stirring of the solution. $^{210}$Po was measured by alpha-particle spectrometry (EG&G Ortec, Oak Ridge, USA). A $^{210}$Pb source was prepared as lead oxalate in the same way as for the calibration source preparation and then measured using LSC for 600 min (200 min × 3 cycles).

**Terms and definitions, symbols, and abbreviations**

In the following, $u(X)$ indicates the uncertainty in quantity $X$:

| $A_T$ and $u(A_T)$ | Certified specific activity of $^{209}$Po tracer on the reference date (Bq g$^{-1}$) | $f_{2\text{-Pb}}$ and $u(f_{2\text{-Pb}})$ | Correction factor for the decay of $^{210}$Pb during the time interval between the separation date and the beginning of the measurement |
| $a_{\text{Pb, std}}$ and $u(a_{\text{Pb, std}})$ | Specific activity of $^{210}$Pb certified standard solution at the reference date (Bq g$^{-1}$) | $f_{3\text{-Pb}}$ and $u(f_{3\text{-Pb}})$ | Correction factor for the decay of $^{210}$Pb during the counting time |
| $a_{\text{Pb, 0}}$ and $u(a_{\text{Pb, 0}})$ | Specific activity of $^{210}$Pb on the sampling date expressed as dry weight (Bq kg$^{-1}$) | $f_p$ and $u(f_p)$ | Correction factor for the decay of $^{209}$Po tracer during the time interval between the reference date of $^{209}$Po and the separation date of Po |
| $a_{\text{Pb, 1}}$ and $u_c(a_{\text{Pb, 1}})$ | Specific activity of $^{210}$Pb on the separation date expressed as dry weight (Bq kg$^{-1}$) | | |
| $a_{\text{Po, 0}}$ and $u_c(a_{\text{Po, 0}})$ | Specific activity of $^{210}$Po on the sampling date expressed as dry weight (Bq kg$^{-1}$) | $f_{2\text{-Po}}$ and $u(f_{2\text{-Po}})$ | Correction factor for the decay of $^{210}$Po during the time interval between the separation of Po and the beginning of the measurement |
| $a_{\text{Po, 1}}$ and $u_c(a_{\text{Po, 1}})$ | Specific activity of $^{210}$Po on the separation date expressed as dry weight (Bq kg$^{-1}$) | $f_{3\text{-Po}}$ and $u(f_{3\text{-Po}})$ | Correction factor for the decay of $^{210}$Po during the counting time |
| $C_{\text{Pb-c}}$ and $u(C_{\text{Pb-c}})$ | Mass fraction of Pb carrier solution (g g$^{-1}$) | $M_{\text{Pb-oxalate}}$ and $u(M_{\text{Pb-oxalate}})$ | Molar mass of lead oxalate (g mol$^{-1}$) |
| $C_{\text{Pb-s}}$ and $u(C_{\text{Pb-s}})$ | Mass fraction of Pb already present in the sample (g kg$^{-1}$) | $M_{\text{Pb}}$ and $u(M_{\text{Pb}})$ | Atomic mass of Pb (g mol$^{-1}$) |
| $\varepsilon$ and $u(\varepsilon)$ | Counting efficiency of $^{210}$Pb | $m_c$ and $u(m_c)$ | Mass of Pb carrier solution added to the sample (g) |
| $f_{\text{A/B}}$ and $u(f_{\text{A/B}})$ | Tailing factor | $m_d$ and $u(m_d)$ | Mass of test portion as a dry weight (kg) |
| $f_g$ and $u(f_g)$ | Mass ratio of atomic mass of Pb to molar mass of Pb-oxalate (PbC$_2$O$_4$) | $m_{\text{f, cal}}$ and $u(m_{\text{f, cal}})$ | Mass of the filter used in the $^{210}$Pb calibration source preparation (g) |



Fig. 2 Typical beta spectra of $^{210}$Pb, $^{210}$Bi, and $^{210}$Po calibration sources: a $^{210}$Pb, $^{210}$Bi, and $^{210}$Po spectra; b pure $^{210}$Bi spectrum

| $m_f$ and $u(m_f)$ | Mass of the filter used for $^{210}Pb$ source preparation of the sample (g) |
| --- | --- |
| $m_{of, cal}$ and $u(m_{of, cal})$ | Total mass of Pb-oxalate plus filter used in the calibration source preparation (g) |
| $m_{of}$ and $u(m_{of})$ | Total mass of the Pb-oxalate precipitate plus filter in $^{210}Pb$ source preparation of the sample (g) |
| $m_P$ and $u(m_P)$ | Mass of $^{209}Po$ tracer added (g) |
| $m_{T, Pb}$ and $u(m_{T, Pb})$ | Mass of $^{210}Pb$ standard solution added (g) |
| $R_{cal}$ and $u(R_{cal})$ | Chemical recovery of Pb in the calibration source preparation |
| $R$ and $u(R)$ | Chemical recovery of Pb in the sample |
| $r_{nA, cal-Bi}$, $r_{nB, cal-Bi}$ and $u(r_{nA, cal-Bi})$, $u(r_{nB, cal-Bi})$ | Net count rates in windows A and B of the $^{210}Bi$ calibration source spectrum (counts $s^{-1}$) |
| $r_{gA, cal-Bi}$, $r_{gB, cal-Bi}$ and $u(r_{gA, cal-Bi})$, $u(r_{gB, cal-Bi})$ | Gross count rates in windows A and B of the $^{210}Bi$ calibration source spectrum (counts $s^{-1}$) |
| $r_{nA}$, $r_{nB}$ and $u(r_{nA})$, $u(r_{nB})$ | Net count rates in windows A and B of the $^{210}Pb$ spectrum of the calibration source or sample (counts $s^{-1}$) |
| $r_{0A}$, $r_{0B}$ and $u(r_{0A})$, $u(r_{0B})$ | Count rates in windows A and B of the blank spectrum (counts $s^{-1}$) |
| $r_{gA}$, $r_{gB}$ and $u(r_{gA})$, $u(r_{gB})$ | Gross count rates in windows A and B of the $^{210}Pb$ spectrum (counts $s^{-1}$) |
| $r_g$, $r_{gt}$ and $u(r_g)$, $u(r_{gt})$ | Gross count rates in the regions of interest (ROIs) of $^{210}Po$ and $^{209}Po$ in the sample spectrum (counts $s^{-1}$) |
| $r_n$, $r_{nt}$ and $u(r_n)$, $u(r_{nt})$ | Net count rates in the ROIs of $^{210}Po$ and $^{209}Po$ in the sample spectrum (counts $s^{-1}$) |
| $r_0$, $r_{0t}$ and $u(r_0)$, $u(r_{0t})$ | Count rates in the ROIs of $^{210}Po$ and $^{209}Po$ in the blank spectrum (counts $s^{-1}$) |
| $t_b$ | Time interval between the reference date of $^{210}Pb$ standard solution and the separation date of Pb (days) |
| $t_{1-Pb}$ | Time interval between the sampling date and the separation date of Pb (days) |
| $t_{2-Pb}$ | Time interval between the separation of $^{210}Pb$ and the beginning of the measurement (days) |
| $t_{3-Pb}$ | Counting time of $^{210}Pb$ in the sample (days) |
| $t_p$ | Time interval between the reference date of $^{209}Po$ tracer and the separation date (days) |
| $t_0$ | Counting time of the blank (s) |
| $t_{1-Po}$ | Time interval between the sampling date and the separation date (days) |
| $t_{2-Po}$ | Time interval between the separation of $^{210}Po$ and the beginning of the measurement (days) |
| $t_{3-Po}$ | Counting time of $^{210}Po$ in the sample (days) |
| $\lambda_b$ and $u(\lambda_b)$ | Decay constant of $^{210}Pb$ (day$^{-1}$) |
| $\lambda_P$ and $u(\lambda_P)$ | Decay constant of $^{210}Po$ (day$^{-1}$) |
| $\lambda_T$ and $u(\lambda_T)$ | Decay constant of $^{209}Po$ tracer (day$^{-1}$) |
| $Z$ and $u(Z)$ | Net count rate corrected for the tailing by ingrowth $^{210}Bi$ in window A of the $^{210}Pb$ spectrum of the calibration source or sample (counts $s^{-1}$) |

## Calculation of the specific activity of $^{210}Pb$

Tailing factor ($f_{A/B}$) and counting efficiency of $^{210}Pb$ in LSC

The $^{210}Pb$ energy region (window A) is interfered with by counts from ingrown $^{210}Bi$. The interference was compensated for by using the ratio of counts in window A to those in window B in a pure $^{210}Bi$ spectrum (the so called "tailing factor": $f_{A/B}$), as shown in Fig. 2b). The tailing factor is independent of the activity level of $^{210}Bi$ in the sample, but is dependent on the quenching level of the sample. As shown in Fig. 3, the quenching levels of the calibrant, the sample, and the reagent blank were kept constant to within $\pm 2\%$ of the relative standard deviation. The tailing factor can be calculated by the following:

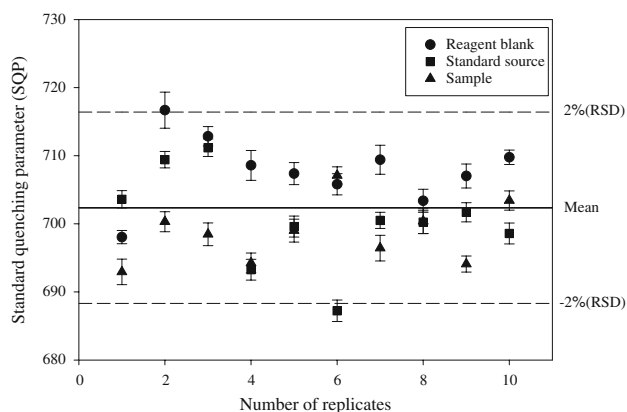$$f_{A/B} = \frac{r_{nA, cal-Bi}}{r_{nB, cal-Bi}} \tag{1}$$

**Fig. 3** Quenching levels of the calibrant, sample, and reagent blank

$$r_{nA,\,cal-Bi} = r_{gA,\,cal-Bi} - r_{0A}$$
$$r_{nB,\,cal-Bi} = r_{gB,\,cal-Bi} - r_{0B} \tag{2}$$

The uncertainty of $f_{A/B}$ is calculated according to:

$$u(f_{A/B}) = f_{A/B} \cdot \sqrt{\left(\frac{u(r_{nA,\,cal-Bi})}{r_{nA,\,cal-Bi}}\right)^2 + \left(\frac{u(r_{nB,\,cal-Bi})}{r_{nB,\,cal-Bi}}\right)^2} \tag{3}$$

$$u(r_{nA,\,cal-Bi}) = \sqrt{u(r_{gA,\,cal-Bi})^2 + u(r_{0A})^2} \tag{4}$$

$$u(r_{nB,\,cal-Bi}) = \sqrt{u(r_{gB,\,cal-Bi})^2 + u(r_{0B})^2} \tag{5}$$

The counting efficiency for $^{210}$Pb and its associated uncertainty can be calculated by Eqs. 6 and 9:

$$\varepsilon = \frac{Z}{R_{cal} \cdot a_{Pb,\,std} \cdot m_{T,\,Pb} \cdot \exp(-\lambda_b \cdot t_b)} \tag{6}$$

$$Z = r_{nA} - r_{nB} \cdot f_{A/B} \tag{7}$$

$$r_{nA} = r_{gA} - r_{0A}$$
$$r_{nB} = r_{gB} - r_{0B} \tag{8}$$

$$u(\varepsilon) = \left\{ \left(\frac{\varepsilon}{Z}\right)^2 \cdot u(Z)^2 + (\varepsilon \cdot t_b)^2 \cdot u(\lambda_b)^2 \right.$$
$$+ \left(-\frac{\varepsilon}{a_{Pb,\,std}}\right)^2 \cdot u(a_{Pb,\,std})^2$$
$$\left. + \left(-\frac{\varepsilon}{R_{cal}}\right)^2 \cdot u(R_{cal})^2 + \left(-\frac{\varepsilon}{m_{T,Pb}}\right)^2 \cdot u(m_{T,Pb})^2 \right\}^{0.5} \tag{9}$$

$$u(Z) = \sqrt{u(r_{nA})^2 + (-f_{A/B})^2 \cdot u(r_{nB})^2 + (-r_{nB})^2 \cdot u(f_{A/B})^2} \tag{10}$$

$$u(r_{nA}) = \sqrt{u(r_{gA})^2 + u(r_{0A})^2} \tag{11}$$

$$u(r_{nB}) = \sqrt{u(r_{gB})^2 + u(r_{0B})^2} \tag{12}$$

Chemical recoveries of Pb in the calibration source and sample

The chemical recovery of lead in the calibration source preparation process was determined gravimetrically using Eq. 13:

$$R_{cal} = \frac{f_g \cdot (m_{of,\,cal} - m_{f,\,cal})}{C_{Pb-c} \cdot m_c} \tag{13}$$

$$u(R_{cal}) = \left\{ \left(\frac{R_{cal}}{f_g}\right)^2 \cdot u(f_g)^2 \right.$$
$$+ \left(\frac{R_{cal}}{(m_{of,cal} - m_{f,cal})}\right)^2 \cdot u(m_{of,cal})^2$$
$$+ \left(-\frac{R_{cal}}{(m_{of,cal} - m_{f,cal})}\right)^2 \cdot u(m_{f,cal})^2$$
$$+ \left(-\frac{R_{cal} \cdot m}{(C_{Pb-c} \cdot m_c)}\right)^2 \cdot u(C_{Pb-c})^2$$
$$\left. + \left(-\frac{R_{cal} \cdot C_{Pb-c}}{(C_{Pb-c} \cdot m_c)}\right)^2 \cdot u(m_c)^2 \right\}^{0.5} \tag{14}$$

In case that the amount of Pb in the sample is not negligible compared with that in the Pb carrier, the sample Pb should be considered in the calculation of the chemical recovery of Pb. The chemical recovery of Pb and its uncertainty in the sample can be calculated by Eqs. 15 and 16, respectively.

In the case of IAEA-326, the amount in the material is 0.016 mg g$^{-1}$ [18], which is much less than the amount of Pb carrier used (30 mg); therefore, it is negligible in the calculation of the chemical recovery of Pb in the sample. In this case, the chemical recovery and its uncertainty in the sample can be calculated by Eqs. 13 and 14:

$$R = \frac{f_g \cdot (m_{of} - m_f)}{C_{Pb-c} \cdot m_c + C_{Pb-s} \cdot m_d} \tag{15}$$

$$u(R) = \left\{ \left(\frac{R}{f_g}\right)^2 \cdot u(f_g)^2 + \left(\frac{R}{(m_{of} - m_f)}\right)^2 \cdot u(m_{of})^2 + \left(-\frac{R}{(m_{of} - m_f)}\right)^2 \cdot u(m_f)^2 + \left(-\frac{R \cdot m_c}{(C_{Pb-c} \cdot m_c + C_{Pb-s} \cdot m_d)}\right)^2 \cdot u(C_{Pb-c})^2 \right.$$
$$+ \left(-\frac{R \cdot C_{Pb-c}}{(C_{Pb-c} \cdot m_c + C_{Pb-s} \cdot m_d)}\right)^2 \cdot u(m_c)^2 + \left(-\frac{R \cdot m_d}{(C_{Pb-c}c + C_{Pb-s} \cdot m_d)}\right)^2 \cdot u(C_{Pb-s})^2$$
$$\left. + \left(-\frac{R \cdot C_{Pb-s}}{(C_{Pb-c} \cdot m_c + C_{Pb-s} \cdot m_d)}\right)^2 \cdot u(m_d)^2 \right\}^{0.5} \tag{16}$$

Mass ratio of the atomic mass of Pb to the molar mass of Pb-oxalate

The mass ratio ($f_g$) of the atomic mass of Pb to the molar mass of Pb-oxalate and its associated uncertainty are calculated using the equations below:

$$f_g = \frac{M_{Pb}}{M_{Pb-oxalate}} \tag{17}$$

$$u(f_g) = f_g \cdot \sqrt{\left(\frac{u(M_{Pb})}{M_{Pb}}\right)^2 + \left(\frac{u(M_{Pb-oxalate})}{M_{Pb-oxalate}}\right)^2} \tag{18}$$

The uncertainty of the molar mass of lead oxalate $u(M_{Pb-oxalate})$ can be derived by combining the standard uncertainties in the atomic masses of its constituents, as shown in Table 1.

Calculation of specific activities of $^{210}$Pb and $^{210}$Po on separation date

The specific activity of $^{210}$Pb and its associated uncertainty on the separation date can be calculated from the LSC measurement, using the following equations:

$$a_{Pb,1} = \frac{Z \cdot f_{2-Pb} \cdot f_{3-Pb}}{m_d \cdot \varepsilon \cdot R} \tag{19}$$

$$f_{2-Pb} = \exp(\lambda_b t_{2-Pb}) \tag{20}$$

$$f_{3-Pb} = \frac{\lambda_b t_{3-Pb}}{1 - \exp(-\lambda_b t_{3-Pb})} \tag{21}$$

The combined uncertainty is the estimated standard deviation equal to the positive square root of the total variance obtained by combining all variance and covariance components using the law of propagation of the uncertainty [5, 6]. The combined uncertainty of the $^{210}$Pb activity is calculated from Eq. 22:

$$u_c(a_{Pb,1}) = \left\{ \left(\frac{a_{Pb,1}}{Z}\right)^2 (r_{nA})^2 + \left(-f_{A/B} \cdot \frac{a_{Pb,1}}{Z}\right)^2 (r_{nB})^2 \right.$$
$$+ \left(-r_{nB} \cdot \frac{a_{Pb,1}}{Z}\right)^2 \cdot u(f_{A/B})^2 + \left(-\frac{a_{Pb,1}}{m_d}\right)^2 (m_d)^2$$
$$+ \left(-\frac{a_{Pb,1}}{\varepsilon}\right)^2 (\varepsilon)^2 + \left(-\frac{a_{Pb,1}}{R}\right)^2 \cdot u(R)^2$$
$$\left. + \left(\frac{a_{Pb,1}}{f_{2-Pb}}\right)^2 \cdot u(f_{2-Pb})^2 + \left(\frac{a_{Pb,1}}{f_{3-Pb}}\right)^2 \cdot u(f_{3-Pb})^2 \right\}^{0.5} \tag{22}$$

$$u(f_{2-Pb}) = f_{2-Pb} \cdot t_{2-Pb} \cdot u(\lambda_b) \tag{23}$$

$$u(f_{3-Pb})$$
$$= f_{3-Pb} \cdot \left\{ 1 - \lambda_b \cdot t_{3-Pb} \cdot \frac{\exp(-\lambda_b \cdot t_{3-Pb})}{1 - \exp(-\lambda_b \cdot t_{3-Pb})} \right\} \cdot \frac{u(\lambda_b)}{\lambda_b} \tag{24}$$

However, if the time interval ($t_{2-Pb}$) between the separation of $^{210}$Pb and the beginning of the measurement and the counting time of the sample ($t_{3-Pb}$) are much smaller than the half-life of $^{210}$Pb (22.2 years), then $f_{2-Pb}$, $f_{3-Pb}$, $u(f_{2-Pb})$, and $u(f_{3-Pb})$ are negligible.

The specific activity of $^{210}$Po on the separation date is calculated by alpha-particle spectrometry, using the ratio of the net count rate of $^{210}$Po to that of $^{209}$Po tracer, and then decay-corrected to the sampling date. As shown in Fig. 4, two decay correction factors ($f_{2-Po}$ and $f_{3-Po}$) were considered for the calculation of the specific activity of $^{210}$Po on

Table 1 Standard uncertainties of atomic weights and the gravimetric factor $f_g$ [19]

| Element | Atomic weight (g mol$^{-1}$) | Quoted uncertainty (g mol$^{-1}$) | Conversion factor | Standard uncertainty (g mol$^{-1}$) | Mass ratio of the atomic mass of Pb to the molar mass of Pb-oxalate | Uncertainty of mass ratio of the atomic mass of Pb to the molar mass of Pb-oxalate |
|---|---|---|---|---|---|---|
| Pb | 207.2152 | 0.00015 | $\sqrt{3}$ | 0.000087 | 0.7019 | 0.000002 |
| C | 12.0107 | 0.0008 | | 0.00046 | | |
| O | 15.9994 | 0.0003 | | 0.00017 | | |

the separation date. The specific activity of $^{210}$Po ($a_{Po,\ 1}$, Bq kg$^{-1}$) expressed as dry weight on the separation date, can be calculated by the following formulae:

$$a_{Po,\ 1} = \frac{A_T \cdot r_n}{m_d \cdot r_{nt}} \cdot m_P \cdot f_p \cdot f_{2-Po} \cdot f_{3-Po} \tag{25}$$

$$r_n = r_g - r_0 \tag{26}$$

$$r_{nt} = r_{gt} - r_{0t} \tag{27}$$

The decay correction factors may be calculated as follows:

$$f_p = \exp\left(-\lambda_T t_p\right) \tag{28}$$

$$f_{2-Po} = \exp\left(\lambda_P t_{2-Po}\right) \tag{29}$$

$$f_{3-Po} = \frac{\lambda_P t_{3-Po}}{1 - \exp\left(\lambda_P t_{3-Po}\right)} \tag{30}$$

The uncertainties associated to the components mentioned above can be calculated as follows:

$$u(r_n) = \sqrt{\frac{r_g}{t_{3-Po}} + \frac{r_0}{t_0}} \tag{31}$$

$$u(r_{nt}) = \sqrt{\frac{r_{gt}}{t_{3-Po}} + \frac{r_{0t}}{t_0}} \tag{32}$$

$$
\begin{aligned}
u(a_{Po,1}) = & \left\{ \left(\frac{a_{Po,1}}{A_T}\right)^2 \cdot u(A_T)^2 + \left(\frac{a_{Po,1}}{r_n}\right)^2 (r_n)^2 \right.\\
& + \left(-\frac{a_{Po,1}}{r_{nt}}\right)^2 \cdot u(r_{nt})^2 + \left(-\frac{a_{Po,1}}{m_d}\right)^2 \cdot u(m_d)^2 \\
& + \left(\frac{a_{Po,1}}{m_P}\right)^2 \cdot u(m_P)^2 + \left(\frac{a_{Po,1}}{f_{2-Po}}\right)^2 \cdot u(f_{2-Po})^2 \\
& \left. + \left(\frac{a_{Po,1}}{f_p}\right)^2 \cdot u(f_p)^2 + \left(\frac{a_{Po,1}}{f_{3-Po}}\right)^2 \cdot u(f_{3-Po})^2 \right\}^{0.5}
\end{aligned}
\tag{33}
$$

$$u(f_p) = f_p \cdot t_p \cdot u(\lambda_T) \tag{34}$$

$$u(f_{2-Po}) = f_{2-Po} \cdot t_{2-Po} \cdot u(\lambda_P) \tag{35}$$

$$
\begin{aligned}
& u(f_{3-Po}) \\
& = f_{3-Po} \cdot \left\{ 1 - \lambda_P \cdot t_{3-Po} \cdot \frac{\exp\left(-\lambda_P \cdot t_{3-Po}\right)}{1 - \exp\left(-\lambda_P \cdot t_{3-Po}\right)} \right\} \cdot \frac{u(\lambda_P)}{\lambda_P}
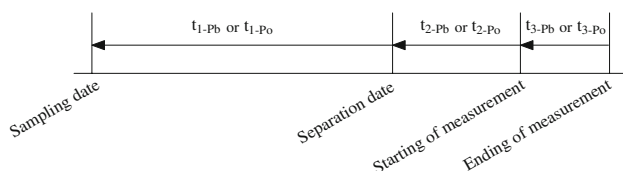\end{aligned}
\tag{36}
$$



Fig. 4 Time intervals between the sampling date, separation date, and measurement date

## $^{210}$Pb and $^{210}$Po in reference soil IAEA-326 on separation date

Relatively few matrix reference materials are available which have been characterized for $^{210}$Pb. For the purposes of testing and illustrating the above procedure, it has been applied to the case of the determination of $^{210}$Pb- and $^{210}$Po-specific activities in reference soil IAEA-326.

The specific activities of $^{210}$Pb and $^{210}$Po corrected to the separation date and its combined uncertainties are summarized in Tables 2 (for $^{210}$Pb) and 3 (for $^{210}$Po). The separation date for these determinations was 22nd October 2007. These data indicate that $^{210}$Pb and $^{210}$Po were in equilibrium on the separation date, as expected.

The recommended values reported for IAEA-326 for $^{226}$Ra and $^{210}$Pb were 32.6 Bq kg$^{-1}$ (95% confidence interval 31.0–34.2) and 53.3 Bq kg$^{-1}$ (48.8–57.8) for the reference date of 31st December 1994, respectively [18]. However, the present-day values will be different from the recommended values due to decay of the original $^{210}$Pb and $^{210}$Po and ingrowth from $^{226}$Ra during the time interval between the reference date and the separation date (Fig. 5). Unfortunately, it is not possible to reliably decay-correct the present-day $^{210}$Pb- and $^{210}$Po-specific activities in IAEA-326 soil to the reference date due to the long time interval between these dates—12.8 years. As this time interval is about 30 times the half-life of $^{210}$Po, it can be expected that $^{210}$Po is now in secular equilibrium with $^{210}$Pb in the material. In addition, it is difficult to estimate the degree of support for $^{210}$Pb from its progenitors in the sample, since there is no guarantee that the $^{222}$Rn from $^{226}$Ra decay in IAEA-326 was quantitatively retained in the soil or in the sample bottle over such a long time interval. Therefore, the results given here are corrected only to the separation date.

The major sources of uncertainty in the measurement result for $^{210}$Pb on the separation date were the uncertainties of net count rates in window A (region of $^{210}$Pb) of the sample spectrum and in window B (region of $^{210}$Bi) of the blank spectrum. The percentage contributions to $(u_c)^2$ of these were 33.2 and 44.3%, respectively. The percentage contributions of the count rates in window A of the blank spectrum and in window B of the sample were both 11%. As predominant uncertainty sources, the percentage contributions to $(u_c)^2$ of count rates in the ROIs of $^{209}$Po and $^{210}$Po were 44.7% and 49.7%, respectively (Table 3).

## Estimation of the relative standard uncertainty of $^{210}$Po on the sampling date

As mentioned above, it is not possible to reliably decay-correct the specific activities of $^{210}$Pb and $^{210}$Po in IAEA-

**Table 2** Quantifying uncertainties in the measurement of $^{210}$Pb in IAEA-326 by LSC

| Symbol | Value of variable | Uncertainty | Conversion factor to standard uncertainty | Standard uncertainty ($u$) | Percentage contribution to $(u_c)^2$ |
|---|---|---|---|---|---|
| $r_{gA}$ (counts s$^{-1}$) | $6.6 \times 10^{-2}$ | $1.9 \times 10^{-3}$ | 1.0 | $1.9 \times 10^{-3}$ | 33.16 |
| $r_{0A}$ (counts s$^{-1}$) | $3.9 \times 10^{-2}$ | $1.1 \times 10^{-3}$ | 1.0 | $1.1 \times 10^{-3}$ | 11.10 |
| $r_{gB}$ (counts s$^{-1}$) | $2.1 \times 10^{-2}$ | $1.0 \times 10^{-3}$ | 1.0 | $1.0 \times 10^{-3}$ | 11.09 |
| $r_{0B}$ (counts s$^{-1}$) | $2.0 \times 10^{-2}$ | $2.0 \times 10^{-3}$ | 1.0 | $2.0 \times 10^{-3}$ | 44.28 |
| $Z$ (counts s$^{-1}$) | $2.6 \times 10^{-2}$ | $3.0 \times 10^{-3}$ | 1.0 | $3.0 \times 10^{-3}$ | 0.00 |
| $f_{A/B}$ | 1.017 | 0.0145 | 1.0 | 0.0145 | 0.005 |
| $m_d$ (kg) | $1.1 \times 10^{-3}$ | $1.0 \times 10^{-7}$ | $\sqrt{3}$ | $5.8 \times 10^{-8}$ | 0.00 |
| $\varepsilon$ | 0.814 | 0.006 | 1.0 | 0.006 | 0.32 |
| $R$ | 0.779 | 0.002 | 1.0 | 0.002 | 0.04 |
| $a_{Pb, 1}$ (Bq kg$^{-1}$) | 38.7 | 5.0* | | | |

*Combined uncertainty

**Table 3** Quantifying uncertainties in the measurement of $^{210}$Po in IAEA-326 by alpha-particle spectrometry

| Symbol | Value of variable | Uncertainty | Conversion factor to standard uncertainty | Standard uncertainty ($u$) | Percent contribution to $(u_c)^2$ |
|---|---|---|---|---|---|
| $r_{gt}$ (counts s$^{-1}$) | $1.0 \times 10^{-2}$ | $2.0 \times 10^{-4}$ | 1.0 | $2.0 \times 10^{-4}$ | 44.7 |
| $r_{0t}$ (counts s$^{-1}$) | $1.6 \times 10^{-5}$ | $9.0 \times 10^{-6}$ | 1.0 | $9.0 \times 10^{-6}$ | 0.07 |
| $r_{g,}$ (counts s$^{-1}$) | $1.2 \times 10^{-2}$ | $2.0 \times 10^{-4}$ | 1.0 | $2.0 \times 10^{-4}$ | 49.7 |
| $r_0$ (counts s$^{-1}$) | $9.3 \times 10^{-4}$ | $1.0 \times 10^{-4}$ | 1.0 | $1.0 \times 10^{-4}$ | 3.98 |
| $A_T$ (Bq g$^{-1}$) | 0.446 | $2.0 \times 10^{-3}$ | 1.0 | $2.0 \times 10^{-3}$ | 1.53 |
| $m_p$ (g) | $9.7 \times 10^{-2}$ | $1.0 \times 10^{-4}$ | $\sqrt{3}$ | $5.8 \times 10^{-5}$ | 0.06 |
| $m_d$ (kg) | $1.0 \times 10^{-3}$ | $1.0 \times 10^{-7}$ | $\sqrt{3}$ | $5.8 \times 10^{-8}$ | 0.00 |
| $\lambda_T$ (day$^{-1}$) | $6.8 \times 10^{-3}$ | $1.5 \times 10^{-5}$ | 1.0 | $1.5 \times 10^{-5}$ | 0.00 |
| $\lambda_P$ (day$^{-1}$) | $5.0 \times 10^{-3}$ | $7.2 \times 10^{-8}$ | 1.0 | $7.2 \times 10^{-8}$ | 0.00 |
| $f_P$ | 0.9166 | 0.0002 | 1.0 | 0.0002 | 0.00 |
| $f_{2-Po}$ | 1.010 | $1.5 \times 10^{-7}$ | 1.0 | $1.5 \times 10^{-7}$ | 0.00 |
| $f_{3-Po}$ | 1.005 | $1.0 \times 10^{-7}$ | 1.0 | $1.0 \times 10^{-7}$ | 0.00 |
| $a_{Po, 1}$ (Bq kg$^{-1}$) | 39.7 | 1.3* | | | |

*Combined uncertainty

**Fig. 5** The uranium decay series
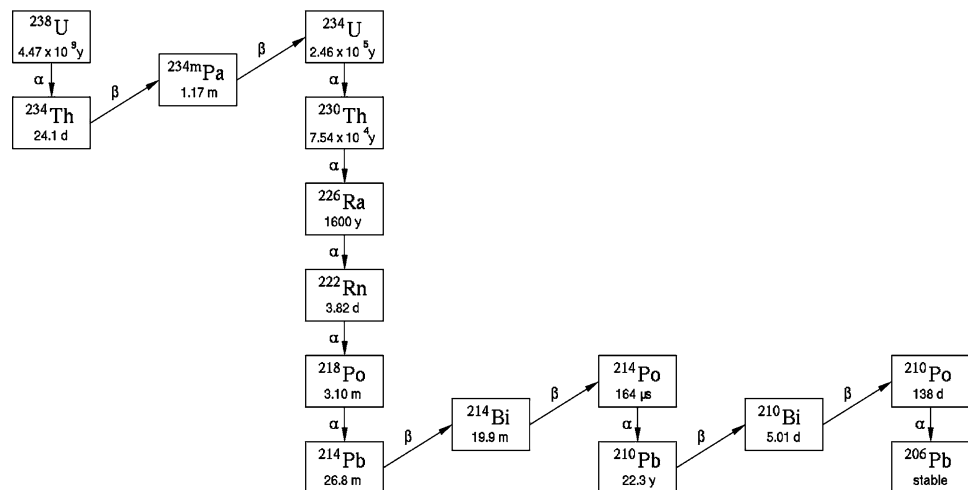
326 determined at the present time to the reference date due to the long time period between the reference and separation dates. This case illustrates that, in order to determine the specific activities in an environmental sample on the sampling date, it is necessary to carry out the analysis within a limited time period after sampling. In this section, we discuss the calculation of results back to the sampling date. The uncertainty of $^{210}$Po calculated to the sampling date can be more significantly affected by the time interval between the separation date and the sampling date in comparison with that of $^{210}$Pb, due to the short half-life of $^{210}$Po (138.38 days). Therefore, we discuss here how the relative standard uncertainty of $^{210}$Po on the sampling date or reference date varies with the time interval between the sampling date and the separation date of Po under some assumptions.

As an example, it was assumed that the specific activity of $^{210}$Pb in the sample on the sampling date was determined to be 50 mBq kg$^{-1}$, with a 13% relative standard uncertainty ($u_c(a_{Pb, 0})/a_{Pb, 0}$), while the relative standard uncertainty ($u_c(a_{Po, 1})/a_{Po, 1}$) of $^{210}$Po-specific activity on the separation date was 3%. In this assumption, only the activity contribution of $^{210}$Pb was considered for the calculation of ingrowth of $^{210}$Po between sampling and separation, because, in most cases, the major contributor to ingrowth over the delay period between sampling and separation is $^{210}$Pb. $^{210}$Bi was assumed to be in secular equilibrium with $^{210}$Pb in the sample.

On the basis of these assumptions, the specific activity of $^{210}$Po and its uncertainty can be decay-corrected to the sampling date by use of the following equation:

$$a_{Po,0} = \left\{ a_{Po,1} - \frac{\lambda_P}{\lambda_P - \lambda_b} a_{Pb,0} \exp(\lambda_b t_{1-Po}) \cdot \left[ \exp(-\lambda_b t_{1-Po}) - \exp(-\lambda_p t_{1-Po}) \right] \right\} \exp(\lambda_p t_{1-Po})$$ (37)

Differentiating Eq. 37, each partial derivative can be calculated as follows:

$$\frac{\partial a_{Po, 0}}{\partial a_{Po, 1}} = I$$ (38)

$$\frac{\partial a_{Po, 0}}{\partial a_{Pb, 0}} = -\lambda_p y$$ (39)

$$\frac{\partial a_{Po, 0}}{\partial \lambda_b} = J\left( t_{1-Po} e^{\lambda_b t_{1-Po}} - y \right)$$ (40)

$$\frac{\partial a_{Po, 0}}{\partial \lambda_p} = a_{Po, 1} t_{1-Po} I - J\left( t_{1-Po} I - \frac{\lambda_b}{\lambda_p} y \right)$$ (41)

where:

$$I = e^{\lambda_b t_{1-Po}}$$

$$J = a_{Pb, 0} \frac{\lambda_p}{\lambda_p - \lambda_b}$$

$$y = \frac{1}{\lambda_p - \lambda_b} \left( I - e^{\lambda_p t_{1-Po}} \right)$$

Therefore, the combined uncertainty of $^{210}$Po concentration (Bq kg$^{-1}$) on the sampling date, $u_c(a_{Po, 0})$ can be calculated by the following formula:

$$u_c(a_{Po,0}) = \left\{ (I)^2 \cdot u\left( a_{Po,1} \right)^2 + (\lambda_p y)^2 \cdot u_c\left( a_{Pb,0} \right)^2 \right.$$

$$+ J^2 \left( t_{1-Po} e^{\lambda_b t_{1-Po}} - y \right)^2 \cdot u(\lambda_b)^2$$

$$\left. + \left[ a_{Po,1} \cdot t_{1-Po} \cdot I - J\left( t_{1-Po} I - \frac{\lambda_b}{\lambda_p} y \right) \right]^2 \cdot u(\lambda_p)^2 \right\}^{0.5}$$ (42)

Figure 6 shows how the relative standard uncertainty for $^{210}$Po on the sampling date changes depending on the time interval between the sampling date and the Po separation date for the example case detailed above. The relative standard uncertainty increases exponentially with the delay time interval. If the $^{210}$Po/$^{210}$Pb activity ratio is 1, then the relative standard uncertainty for $^{210}$Po corrected to the sampling date reaches 10% for a sampling-separation delay period of 100 days. However, in the case that the ratio is 0.1 (a typical ratio in rain water [1, 13]), a 10% relative standard uncertainty for $^{210}$Po is reached after only 13 days (Fig. 4), while in the case that the ratio is 10 (a typical ratio in molluscs and the soft tissue of bivalves [14, 15]), the relevant time period is 400 days from the sampling date (Fig. 6).

As mentioned above, in these calculations, $^{210}$Bi was assumed to be in secular equilibrium with $^{210}$Pb in the sample. This is not always the case however. For example, in rainwater, the $^{210}$Bi/$^{210}$Pb activity ratio is normally less than 1. In most cases, this assumption causes only small errors. However, it should be kept in mind that, for some sample types where extreme disequilibrium may occur (for example, process waters from the mining industry), additional correction factors may be required. In any case, the introduction of both quantifiable and unquantifiable errors may be reduced by the minimization of the time delay between sample collection and analysis. In other words, it is good practice to keep the delay period as short as practicable.
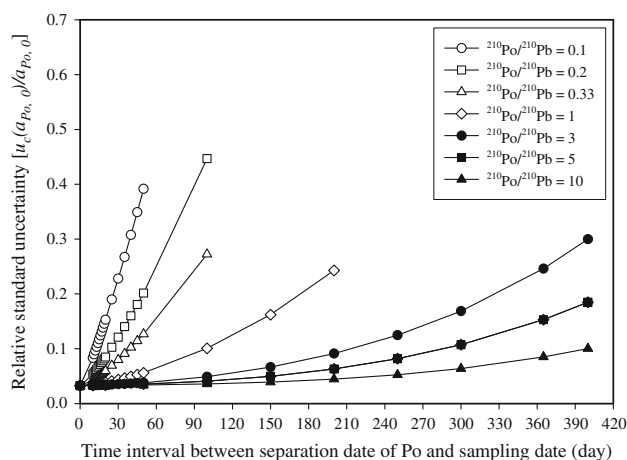
**Fig. 6** The variation of the relative standard uncertainty ($u_c(a_{\text{Po, 0}})/a_{\text{Po, 0}}$) of $^{210}$Po on the sampling date with the time interval between the separation date and the sampling date for several $^{210}$Po/$^{210}$Pb activity ratios

## Conclusions

In this work, the quantification of measurement uncertainties in the determination of $^{210}$Pb- and $^{210}$Po-specific activities, including the correction of $^{210}$Pb- and $^{210}$Po-specific activities to the sampling (or reference) date under some assumptions, was elaborated. The variation of the relative standard uncertainty of $^{210}$Po-specific activity on the sampling date with the time interval between the sampling date and the separation date was evaluated.

The methods described in this paper were applied to an example analysis of reference soil IAEA-326. The major sources of uncertainty in the measurement result of $^{210}$Pb on the separation date were the uncertainties of the net count rates in window A of the sample spectrum and in window B of the blank spectrum. The predominant sources of uncertainty in the measurement of $^{210}$Po were also the uncertainties of the net count rates in the ROIs of $^{209}$Po and $^{210}$Po.

The relative standard uncertainty of the $^{210}$Po determination can be significantly affected not only by the time interval between the reference date and the separation time of Po but also by the $^{210}$Po/$^{210}$Pb activity ratio, i.e., the ratio of their respective specific activities. In general, the time delay between sample collection and $^{210}$Po determination should be kept as short as practicable in order to avoid errors due to ingrowth and decay, particularly for sample types for which the $^{210}$Po/$^{210}$Pb activity ratio may be low.

## References

1. Tokieda T, Narita H, Harada K, Tsunogai S (1994) Sequential and rapid determination of Po-210, Bi-210 and Pb-210 in natural waters. Talanta 41:2079–2085. doi:10.1016/0039-9140(94)00182-0
2. Craig H, Krishnaswami S, Somayajulu BLK (1973) $^{210}$Pb–$^{226}$Ra: radioactive disequilibrium in the deep sea. Earth Planet Sci Lett 17:295–305. doi:10.1016/0012-821X(73)90194-5
3. United Nations Scientific Committee on the Effects of Atomic Radiation (UNSCEAR) (2000) Sources and effects of ionizing radiation. 2000 Report to the General Assembly, with scientific annexes. United Nations, New York
4. Shakhashiro A, Gondin Da Foseca Azeredo AM, Sansone U, Kim C-K, Kis-Benedek G, Trinkl A, Benesch T, Schorn R (2006) Report on the IAEA-CU-2006-02 proficiency test on the determination of $^{137}$Cs and $^{210}$Pb in spiked soil. IAEA/AL/166
5. IAEA (2008) Report on the IAEA-CU-2007-09 world-wide open proficiency test for the determination of $^{210}$Po in water. IAEA/AL/183 (in press)
6. Matthews KM, Kim C-K, Martin P (2007) Determination of $^{210}$Po in environmental materials: a review of analytical methodology. Appl Radiat Isot 65:267–279. doi:10.1016/j.apradiso.2006.09.005
7. Fleer AP, Bacon MP (1984) Determination of $^{210}$Pb and $^{210}$Po in seawater and marine particulate matter. Nucl Instrum Methods Phys Res A 223:243–249. doi:10.1016/0167-5087(84)90655-0
8. BIPM IEC, IFCC, ISO, IUPAC, IUPAP, OIML (1995) Guide to the expression of uncertainty in measurement. International Organization for Standardization, Geneva
9. Ellison SLR, Rosslein M, Williams A (2000) Quantifying uncertainty in analytical measurement, EURACHEM/CITAC
10. IAEA-TECDOC-1401 (2004) Quantifying uncertainty in nuclear analytical measurements. International Atomic Energy Agency, Vienna, Austria
11. García-Orellana I, García-Leon M (2002) An easy method to determine $^{210}$Po and $^{210}$Pb by alpha spectrometry in marine environmental samples. Appl Radiat Isot 56:633–636. doi:10.1016/S0969-8043(01)00261-5
12. Vreček P, Benedik L (2003) Evaluation of measurement uncertainty in the determination of $^{210}$Pb and $^{210}$Po using beta counting and alpha spectrometry. Accredit Qual Assur 8:134–137. doi:10.1007/s00769-002-0577-5
13. Parfenov YD (1974) Polonium-210 in the environment and in the human organism. At Energy Rev 12:75–143
14. Stepnowski P, Skwarzec B (2000) A comparison of $^{210}$Po accumulation in molluscs from the southern Baltic, the coast of Spitsbergen and Sasek Wielki Lake in Poland. J Environ Radioact 49:201–208. doi:10.1016/S0265-931X(99)00094-6
15. Guogang J, Belli M, Sansone U, Rosamilia S, Blasi M (2003) $^{210}$Pb and $^{210}$Po concentrations in the Venice lagoon ecosystem (Italy) and the potential radiological impact to the local public and environment. J Radioanal Nucl Chem 256:513–528. doi:10.1023/A:1024512118760
16. Smith-Briggs JL, Bradley EJ, Potter MD (1986) The ratio of lead-210 to polonium-210 in U.K. diet. Sci Total Environ 54:127–133. doi:10.1016/0048-9697(86)90260-3
17. Vajda N, LaRosa J, Zeisler R, Danesi P, Kis-Benedek Gy (1997) A novel technique for the simultaneous determination of $^{210}$Pb and $^{210}$Po using a crown ether. J Environ Radioact 37:355–372. doi:10.1016/S0265-931X(95)00059-J

18. Bojanowski R, Radecki Z, Campbell MJ, Burns KI, Trinkl A (2001) Report on the intercomparison run for the determination of radionuclides in soils IAEA-326 and IAEA-327. IAEA/AL/100

19. de Laeter JR, Böhlke JK, De Bièvre P, Hidaka H, Peiser HS, Rosman KJR, Taylor PDP (2003) Atomic weights of the elements. Review 2000 (IUPAC technical report). Pure Appl Chem 75:683–800. doi:10.1351/pac200375060683